

We are IntechOpen, the world's leading publisher of Open Access books Built by scientists, for scientists

6,400

Open access books available

174,000

International authors and editors

190M

Downloads

Our authors are among the

154

Countries delivered to

TOP 1%

most cited scientists

12.2%

Contributors from top 500 universities



WEB OF SCIENCE™

Selection of our books indexed in the Book Citation Index
in Web of Science™ Core Collection (BKCI)

Interested in publishing with us?
Contact book.department@intechopen.com

Numbers displayed above are based on latest data collected.
For more information visit www.intechopen.com



Chapter

Impulse Measurement Methods for Space Micro-Propulsion Systems

Yang Ou, Yuqi Li, Yu Zhang, Jianjun Wu and Yuqiang Cheng

Abstract

Space micro-propulsion systems are increasingly considered an attractive option for station-keeping and drag-makeup purposes for the mass- and power-limited satellites due to their critical factors of simple design, small volume, and high specific impulse. These systems typically generate low-range thrust from nN to mN, and their impulses are less than mNs, making it difficult for conventional sensors to detect them directly. Consequently, the design of a special thrust stand is often necessary to measure these micro-propulsion systems. This chapter outlines recommended practices for the operation and calibration of three conventional measurement methods, along with the introduction of an impulse measurement stand developed at the National University of Defense Technology. The chapter presents the fundamentals, calibration method, and experimental results of the stand operation, while also analyzing error sources. Finally, the chapter discusses the demand and direction of micro-impulse measurement development.

Keywords: micro-propulsion system, impulse measurement, pendulum stand

1. Introduction

With the gradual refinement of the functions of satellite networking and space-based network information systems, the requirements for the propulsion system necessary for satellite missions are further increased [1–3]. Compared with the traditional chemical propulsion system, the electric propulsion system has the advantages of high specific impulse, lightweight, and long lifespan, so it gradually becomes a better scheme for satellite attitude control, orbit transformation, and drag compensation [1, 3, 4].

Electric thrusters are available in a plethora of types, each boasting unique operating principles and characteristics. Regardless of the specific type employed, however, all electric thrusters must undergo three essential steps: design, trial production, and testing. For the electric thruster, it needs not only the test link to evaluate and verify the function and performance, but also the test link to expose the thruster development issues and seek potential solutions. Therefore, the pre-research, pattern, prototype, and flight application stages of the electric propulsion system development are inextricably linked to the testing and measurement technology, which serves as an indispensable cornerstone of electric propulsion [5, 6].

Unlike chemical and cold air propulsion systems, electric propulsion systems typically require a vacuum environment for ignition testing and operation. Consequently, creating a high vacuum environment artificially becomes necessary during ground testing of electric propulsion. The research on electric propulsion encompasses development, testing, identification, and application, and the testing of electric propulsion systems runs through all aspects of scientific research.

There are numerous topics covered in electric propulsion testing, and some overlap between them, but the purpose of the testing is relatively clear, which can be divided into five categories according to the intended purpose [5, 6]:

1. Ignition test. The electric propulsion ignition test is a crucial means of obtaining important information about electric propulsion, including ignition start and steady-state operation tests. The ignition start test verifies successful and reliable ignition of the electric thruster, while the steady-state operation test ensures stable operation for a short time or a long time based on the ignition start test.
2. Performance measurement test. After ensuring the stable operation of the electric thruster, it is necessary to measure its performance parameters such as thrust, efficiency, specific impulse, and beam divergence angle to complete the evaluation of the comprehensive performance of the electric thruster.
3. Life test. The ground test was conducted to verify whether the accumulated working time and switching times of the electric thruster meet the design index or the requirements of the space mission.
4. Plasma diagnostics. Through an analysis of the plasma state of the electric thruster, it is possible to optimize the structural design of the thruster and evaluate the potential impact of the plume on the spacecraft.
5. Environmental adaptability test. Ensure that the reliability of the electric thruster meets the requirements of the ground test conducted in the satellite launch and on-orbit working environment, and verify the performance under the current working conditions.

Among the above five types of tests, the performance measurement test with micro-thrust and impulse measurement as the core is the main test item of the electric propulsion system. This measurement is an essential measurement link to evaluate the performance of the electric propulsion system and is also an important reference index to measure the stability of the electric propulsion system, which runs through all stages of the spacecraft, such as the single machine level, subsystem level, and the whole star level [7–10].

Combined with the principle, working environment, and thrust level of the electric thruster, the micro-thrust and impulse measurement test for the electric thruster have the following characteristics:

1. Small impulse. At present, the thrust range of commonly used electric thrusters, such as Hall thrusters and ion Hall thrusters, covers from micro-newton to nano-newton, while the impulse element of pulse-working electric thrusters generally ranges from micro-newton to milli-newton. Therefore, the micro-thrust and impulse measurement system needs to capture weak mechanical signals in small

time scales, and the measurement system needs to have high sensitivity, resolution, and anti-interference ability.

2. Low thrust–weight ratio. The thrust–weight ratio is the ratio of thrust to weight of an electric thruster. The thrust of the electric thruster is small, and the weight is large. Its thrust–weight ratio is usually between 10^{-7} and 10^{-3} , which is far less than that of the chemical propulsion system. Too low a thrust–weight ratio will lead to a negligible additional weight component that must be eliminated or suppressed; otherwise, it will bring obvious interference and error to the measurement of a small thrust or impulse. In addition, the sensitivity and load-bearing capacity of the measuring platform is often difficult to be compatible with. How to ensure that the resolution and sensitivity of the electric thruster can be improved as much as possible under the normal installation is always the core issue of micro-thrust and impulse measurement.
3. Measurement in a vacuum environment. Electric thrusters usually need to work in a vacuum environment, so the materials, components, sensors, and other equipment required for thrust measurement need to have the ability to work in a vacuum.
4. Interference factors. The thrust of the electric thruster is usually in the range of microns to microns, and the impulse element is in the range of microns to microns. Any small vibration and interference will affect the measurement. The key is to avoid the interference of cables and gas pipes, vibration interference, thermal impact, and electromagnetic interference.

2. Impulse measuring principle

The basic principle behind most existing measurement methods is to apply the thrust or impulse to be measured on the measuring platform, establish the functional relationship between the thrust and impulse, and the corresponding physical effect according to the mechanical response results of the measuring platform (e.g., vibration amplitude and rotation angle), and then calibrate the functional relationship through the standard force, thereby achieving the quantitative measurement of thrust and impulse. In electric thrusters, the key to micro-thrust and impulse measurement is to measure the variation of thrust with time. For thrusters operating in a transient state (e.g., pulsed plasma thrusters), the thrust action time is very short, and it is unnecessary or impossible to measure the variation of thrust with time. In this case, the thrust action effect can be expressed by impulse, which is also the impulse measurement [11–13].

2.1 Classification

At present, the commonly used methods for measuring thrust and impulse include the deformation structure method, balance method, torsion pendulum method, and cantilever beam method. According to the different mechanical response results of the thrust platform, they can be divided into the direct transfer measurement method, pendulum force measurement method, and target transfer measurement method.

2.1.1 Direct transfer measurement

The direct transfer measurement method refers to that the thruster being fixed directly on the force-measuring sensor or the thrust generated by the thruster being directly applied to the force-measuring sensor through the measuring platform. During the measurement, the thrust and impulse are identified by the sensor. This method is suitable for thrust measurement environments with large thrusts, such as chemical thrusters, electric arc thrusters, and resistance heating thrusters. The key to measurement is the measurement sensor. The commonly used sensors include a piezoelectric sensor, strain gauge sensor, and capacitance sensor [5, 13].

The direct transfer measurement method is the preferred method for large thrust measurement. Its structure is relatively simple, and the measurement process is simple and fast. However, when the thrust magnitude is small, the mechanical signal is susceptible to be disturbed by environmental noise and mechanical vibration. This makes it difficult for the sensor to capture the weak mechanical signal.

2.1.2 Measurement method of swing force

In the pendulous force measurement method, the thruster is mounted directly on the measuring platform, which can measure the thrust and impulse of the thruster with a small force. The measurement accuracy and resolution are high, which is the current mainstream scheme of the thrust and impulse measurement of the electric thruster. As shown in **Figure 1**, the swing force measurement process essentially uses the thrust of the thruster to excite the pendulum structure bench and obtains the thrust or impulse in reverse calculation by calibrating the relationship between the motion law of the pendulum structure bench to the thrust or impulse [14, 15].

The specific implementation of the swing force measurement method includes closed-loop and open-loop measurement methods. In the closed-loop measurement, the electromagnetic force is used to compensate for the effect of the thrust so that the measurement platform is in the random equilibrium and the electromagnetic force equals to the thrust [16]. The closed-loop measurement method can eliminate the interference of gravity and material rigidity on the measurement, and the

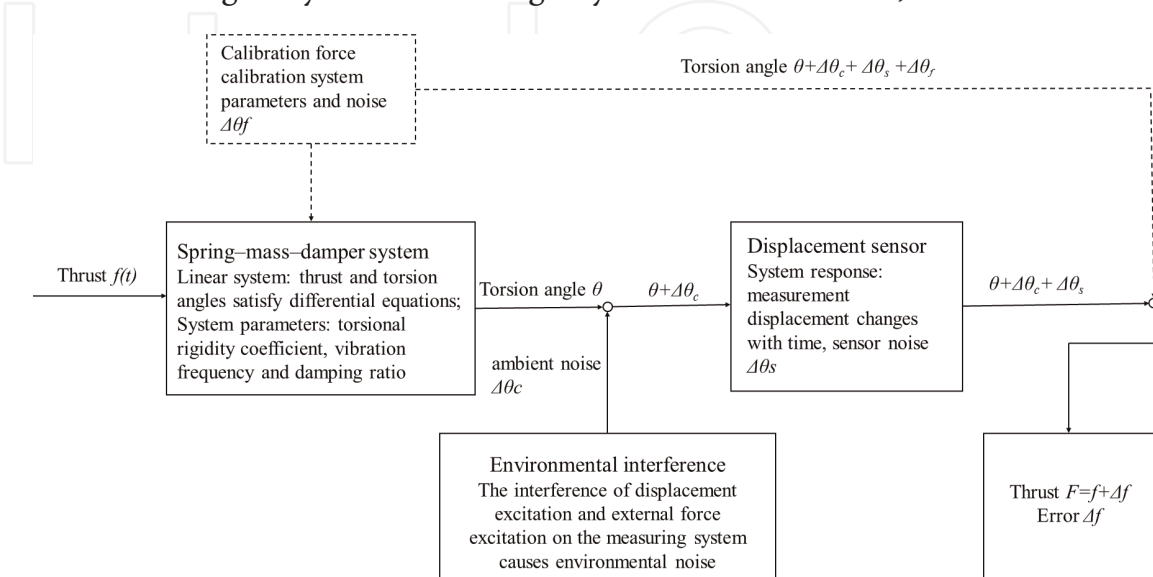


Figure 1. Measurement principle of swing force.

measurement results are relatively more accurate. The open-loop measurement method usually records the position change of the pendulum and then calculates the thrust and impulse through the calibration of the standard force. The commonly used sensors for measuring the change of pendulum position include a laser displacement sensor, capacitance displacement sensor, laser angle sensor, and photoelectric sensor. In addition, to control the motion of the pendulum and quickly return to the equilibrium state after the measurement, the pendulum force measurement device is usually equipped with the corresponding dampers.

According to the structural form of the pendulum, the pendulum force measurement methods can be divided into three types: suspended pendulum, inverted pendulum, and torsion pendulum, as shown in **Figure 2**. Although the three structures are slightly different, they can be considered a “spring-mass-damper” system [9].

2.1.3 Target transfer measurement method

The target transfer measurement method is to impact the plume from the thruster on the target and calculate the thrust of the thruster by measuring the position change of the target under the impact force. **Figure 3** shows the schematic diagram of a typical target transfer measurement scheme, which consists of target, elastic beam, displacement sensor, and calibration device. The elastic beam with minimum rigidity is fixed with the target with maximum rigidity. When the plume from the thruster impacts the target, the elastic beam will deflect obviously, and the displacement sensor can measure the horizontal displacement of the elastic beam. Calibrate the horizontal displacement and standard force of the elastic beam through the calibration device, establish the corresponding functional relationship, and realize the accurate measurement of different thrust sizes. Most target structures are equivalent to simple pendulum structures, and their motion characteristics are similar to the pendulum force formula [17, 18].

Compared with the other two kinds of measurement methods, the target transfer measurement method is a non-contact indirect measurement, which can avoid the impact of measurement and control cable, thruster working noise, and vibration on the measurement results to a certain extent [5, 13, 16]. In addition, the target transfer measurement method has a simple structure and is easy to install and

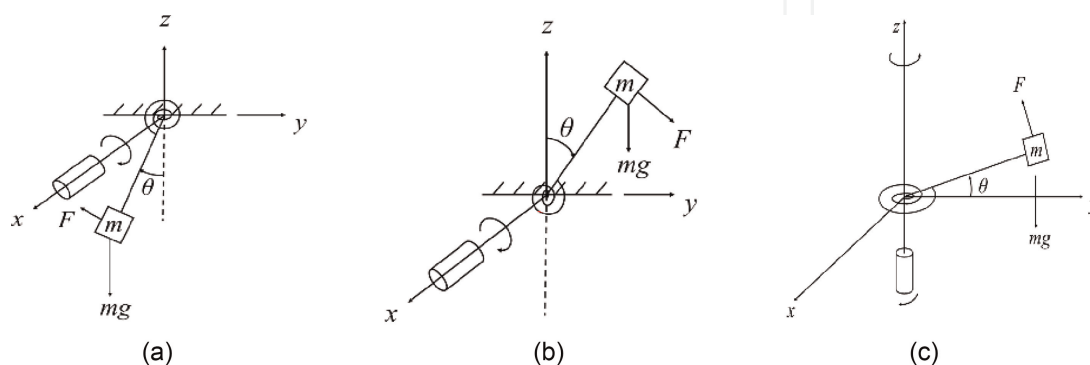


Figure 2. Spring-mass-damper system. (a) Hanging pendulum, (b) inverted pendulum and (c) torsional pendulum.

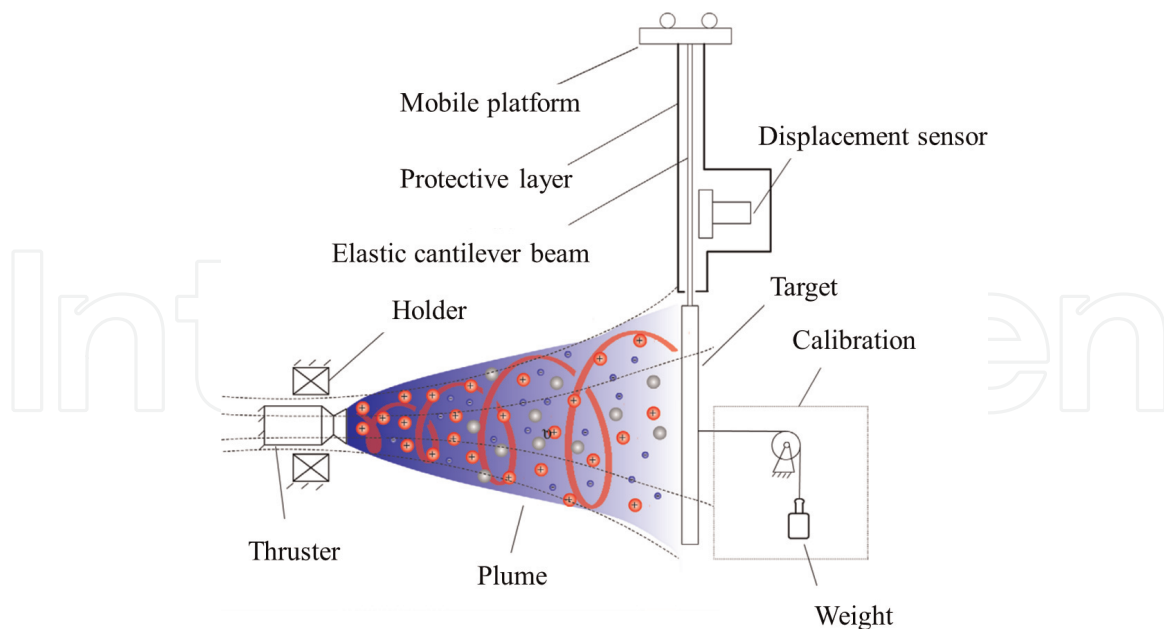


Figure 3.
Schematic diagram of a typical target transfer measurement.

implement. However, due to the effectiveness and secondary effects of the plume, the error is relatively large. The key points are as follows:

1. The plume is unable to ensure that all impacts are on the target and the actual impact level is less than the theoretical generation;
2. For the transient thruster operation, the motion of the plume has greater randomness, and the single impact force fluctuates greatly;
3. After the target impact, part of the plume will rebound, resulting in a larger measured value than the actual value;
4. The angle deviation of the elastic target is inevitable after being impacted, and the impact force of the plume will be partially lost [7, 11, 19, 20].

2.2 Calibration

At present, the principle of the mainstream measuring platform is almost based on the effect of force. The thrust is obtained by determining the basic parameters of the vibration system and measuring the displacement response of the vibration components and then by inversion according to the dynamic equation. The determination of the basic parameters of the vibration system is the calibration process, which applies a constant calibration force or calibration impulse to the measuring platform and then determines the system parameters according to the obtained system response and dynamic relationship [5]. Although the dynamic function can be calculated theoretically by obtaining the correlation coefficient of the measuring platform, it is more convenient, intuitive, and reliable to determine the system parameters through the calibration process.

In the process of micro-thrust and impulse measurement, the calibration process is indispensable. The first is to establish the functional relationship between thrust or impulse and displacement through the calibration process. The second is to determine the accuracy, repeatability, stability, and sensitivity of the measuring device by repeatedly loading the standard known force. The third is to avoid system error by comparing and correcting the measured value and theoretical value. Therefore, the repeatability, operability, adjustability, stability, and accuracy of the calibration device is one of the key technologies to ensure the performance of the micro-thrust measurement system and also an important basis to verify its measurement level.

According to whether the calibration force generation device is in direct contact with the measuring device, the calibration method can be divided into contact type and non-contact type. The contact calibration method includes the weight method and the impact hammer. The principle of the weight method is simple and easy to operate, but it is easy to be affected by sliding friction, air resistance, elastic expansion, and drag of the rope and limited by the minimum weight; it is difficult to provide high-precision micro-newton calibration force. The pendulum method uses a pendulum with a known mass to impact the measuring bench from a certain height to form an impulse with a known size. This method is also simple and easy to operate, but the error is large and difficult to control [12, 13, 21]. Non-contact calibration methods include the electrostatic comb method and the electromagnetic force method. The electrostatic comb method is usually composed of a group of interlocking non-contact comb teeth separated at very small intervals. The electrostatic repulsion force generated when approaching is used as the calibration force. It can not only provide a stable thrust but can also generate a high-accuracy impulse by controlling the number of comb charges and voltage application time. The electromagnetic force calibration method uses the magnetic effect of a current or the theorem of ampere force to generate a stable electromagnetic force, including the combination of a coil with a permanent magnet and the combination of an electromagnet with an energized wire. Similar to the electrostatic comb method, the electromagnetic force method can also generate stable calibration force and can also accurately generate calibration impulses of known size. In addition, the electromagnetic force is not easily affected by the external power supply line, and its accuracy is higher than that of the electrostatic comb method [22–24].

2.3 Performance metrics

The main technical indicators of the micro-thrust and impulse measurement platform include sensitivity, stability, accuracy, resolution, and response time.

2.3.1 Sensitivity

As the core technical index of the measuring platform, sensitivity, accuracy, and resolution are closely related, the definition of sensitivity in micro-thrust and impulse measurement is slightly different. Generally speaking, the sensitivity of steady-state micro-thrust measurement is the offset that the platform can achieve under a given thrust. As shown in Formula (2.7), the sensitivity is related to the length of the moment arm and the elastic coefficient and is regarded as the key index of the mechanical design of the measuring bench [5, 9].

2.3.2 Stability

In the process of micro-thrust and impulse measurement, it is necessary to ensure that the response of the measuring bench is consistent and repeatable; otherwise, the calibration will be meaningless, and the accuracy and accuracy of the measurement cannot be guaranteed. In addition, long-term measurement needs to ensure the long-term stability of the bench. There are two main factors that affect the repeatability of measurement. One is the zero drift, that is, the change of zero point or the actual position of the pendulum, and the other is the gain drift, that is, the change of response coefficient or elasticity coefficient. The temperature change or friction of mechanical or electronic components and elastic components will cause drift. In order to pursue the accuracy of measurement, the generation of drift should be avoided as much as possible [9, 21].

2.3.3 Resolution

Resolution is defined as the minimum difference in the response of the measuring platform after being loaded by two different thrusts or impulses. Resolution is the ability of the measuring platform to distinguish the mechanical effects of loading and is also a measure of the minimum value of thrust and impulse change of the measuring platform. The noise level of the measuring platform is directly related to the resolution, and high resolution can be achieved by minimizing the noise. In the process of micro-thrust and impulse measurement, the noise sources usually include the electrical noise of the sensor, the mechanical noise caused by environmental vibration, and the response change caused by the periodic change of temperature.

The resolution of the measuring bench can be quantified by continuously changing the magnitude of the loading force until the response cannot be resolved. However, in the actual measurement process, the error of this method is relatively large. Usually, the resolution is determined according to the measurement noise level, and the resolution can be specified to be twice the noise signal. The noise signal can be characterized by the ratio between amplitude and frequency or power spectral density [5, 8, 9, 25].

In the measurement process of an electric thruster, unless some measurement methods specifically use the resonance principle, the natural frequency between the electric thruster and the measuring platform should generally be avoided, so as to prevent the generation of resonance. In addition, to ensure the accuracy of measurement, the noise of the bench must be far less than the range of the thruster that can be produced by the thruster.

2.3.4 Response time

The response time of the measuring bench is an important indicator of dynamic measurement, which can be characterized by many parameters, such as rise time (the time required for the response to reach 100% of the steady-state value), peak time (the time required for the response to reach the peak value), and stability time (the time required for the response to change less than 2% near the steady-state value) [9].

2.3.5 Accuracy

Accuracy is a measure of the error between the measured value and the true value of the measuring bench. For a high-performance measuring bench, it is not only required to be sensitive enough, the results have obvious repeatability, not affected by

random errors, but also to ensure the measurement results [16]. In the measurement process, the system error is usually minimized to improve the measurement accuracy, and the accuracy needs to be calibrated through standard thrust and impulse. In addition, the calibration method needs to be strictly designed to avoid introducing new system errors.

3. Impulse measurement stand in NUDT

Since 1960s, researchers across the countries both domestically and internationally have successively developed various micro-thrust/micro-impulse measurement devices, including balance, single pendulum, double pendulum, torsion pendulum, and cantilever beam. The measuring range of these devices is mostly in the millinewton scale, and some attempts have also been conducted for the lower scale. Based on the inverted pendulum structure, NASA uses capacitive displacement sensors and gravity accelerometers to detect the position change of the swing arm and then measure the thrust, which can achieve 0–700 μN measurement range, and the noise is less than 1 $\mu\text{N}/\text{Hz}$ [26]. Researchers at the University of the Witwatersrand improved the torsion pendulum, which can achieve micro-newton thrust and 0.27–600 μN , the error of impulse measurement in the range of Ns is less than 4% [27]. NASA also developed a single-end fixed torsion wire suspension torsion pendulum, with a resolution of 25nN and a force measuring range of 100 nN \sim 500 μN . The error is less than 25% [28]. Researchers at the University of Tokyo in Japan has developed an elastic pivot type non-equal arm torsion pendulum with a resolution of 0.7 $\mu\text{N}\cdot\text{s}$ impulse measurement [29]. Researchers at Huazhong University of Science and Technology have achieved a resolution of 0.09 μN with a maximum range of 264 μN micro-thrust measurement and a resolution of 0.47 $\mu\text{N}\cdot\text{s}$ with a maximum range of 1350 $\mu\text{N}\cdot\text{s}$ through a special suspension and torsional balance design for the torsional pendulum [30]. Although the measurement of thrust and impulse at the level of millinewton has reached a high level, there are still many difficulties in the measurement of thrust and impulse at the level of micro-nano or even nano-nano. For example, there is noise in the measuring instrument itself and the environment, which often submerges the measured signal and greatly affects the measurement accuracy. At the same time, when the micro-thruster works, the measuring platform will vibrate under the force, which will also affect the measuring accuracy. In addition, the vacuum pumping process will also have adverse effects on the vacuum chamber and internal measuring system. These difficulties lead to less thrust and impulse measurement methods of micro-newton magnitude and low accuracy. At the same time, it is extremely difficult for the existing international measurement technology to meet the requirements of integrated thrust/impulse measurement with a large range, high resolution, and high accuracy at the same time.

In order to realize the integrated measurement of micro-impulse, the National University of Defense Technology (NUDT) has built a C-tube torsion micro-impulse measurement method and a direct calibration method based on ampere force, which has solved the problems of weak signal sensing, anti-interference and anti-randomness, and online calibration, and developed a C-tube torsion micro-impulse measurement device and online calibration system as shown in **Figure 4**. The theoretically achievable micro-impulse measurement range is 100 nNs–100 mNs, The micro-thrust measurement range is 100 nN–100 mN, providing a necessary device for the development and engineering application of micro-nano satellite propulsion systems.

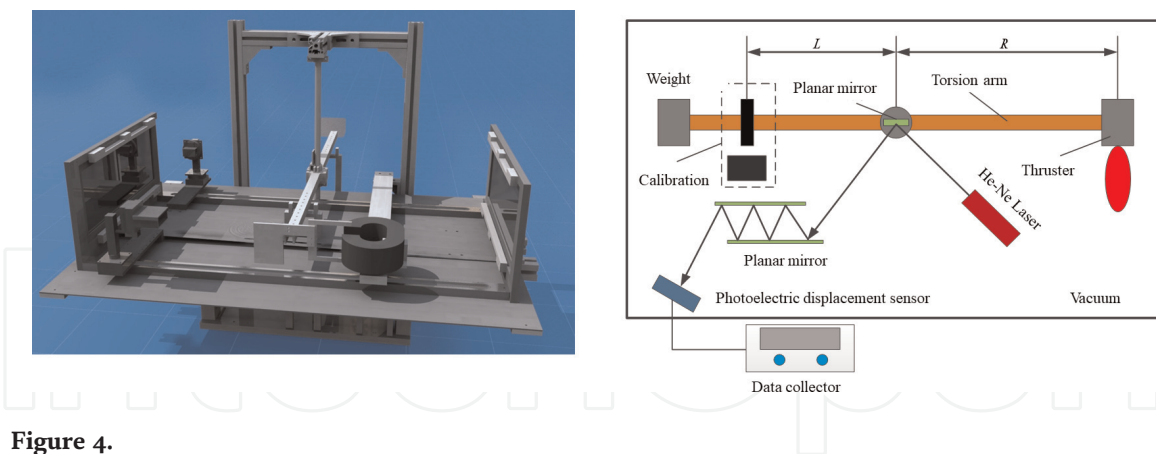


Figure 4.
C-tube torsion micro-impulse measurement device.

3.1 Fundamental theory

The C-tube torsion pendulum micro-impulse measurement system can be divided into the following subsystems: (1) displacement signal optical measurement subsystem, including He-Ne laser, planar mirror array, and photoelectric displacement sensor (PDS); (2) torsion pendulum structural parts, including torsion bar, swing arm, bracket, connecting parts, etc.; (3) damping and electromagnetic calibration subsystem, including several electromagnetic coils, permanent magnets, control circuits, etc. [21].

As shown in **Figure 4**, when the thruster works, its impulse will act on the torsion pendulum system. When the thruster works, its impulse will act on the swing arm and drive the torsion bar to rotate. The reflector installed on the swing arm reflects the laser beam emitted by the He-Ne laser to the remote PDS photosensitive surface. With the action of the impulse, the light spot produces a small displacement on the PDS photosensitive surface, which makes the PDS produce a small voltage signal output. Therefore, by calibrating the relationship between the impulse and the micro voltage signal, the corresponding micro-impulse can be calculated using the voltage signal.

The elastic element of the torsion pendulum is the key component of the torsion pendulum measurement system, which determines the mechanical response characteristics of the torsion pendulum, and is also an important component that affects the measurement performance of the torsion pendulum. According to the knowledge of engineering mechanics, it can be proved that within the elastic range of the material, the torsional deformation of the metal C-tube is strictly linear with the magnitude of the axial torque it is subjected to. The C-tube torsion pendulum measurement system uses this linear relationship to measure the impulse.

Assume that the wall thickness of the C-shaped tube is t , the length is l , the length of the cross-section centerline is m , the material shear modulus of elasticity is G , the rotational inertia of the torsion pendulum relative to the axis of the C-shaped tube is I , the impulse generated by the propulsion system is micro I_s , and the instantaneous rotational angular velocity of the torsion pendulum beam is w . When the torque T is loaded on the C-shaped tube, the torsional deformation generated is [31]:

$$T = \frac{2Gmt^3}{3l} \alpha \quad (1)$$

where α is the torsion angle of the C-shaped pipe under the action of torque. By integrating formula (1), the rotation angle of the C-tube torsion beam can be obtained α_0 , and its stored energy is [31]:

$$E = \int_0^{\alpha_0} T d\alpha = \int_0^{\alpha_0} \frac{2Gmt^3}{3l} \alpha d\alpha = \frac{Gmt^3 \alpha_0^2}{3l} \quad (2)$$

The motion of the torsion pendulum is fixed axis rotation, and its instantaneous kinetic energy is $I\omega^2/2$. When the impulse I_s acts on the torsion pendulum, the torsion pendulum starts to move. In the first quarter period of its movement, it can be considered that the energy is converted between the rotational kinetic energy of the torsion pendulum and the elastic potential energy stored in the C-tube, that is, the energy consumed by the C-tube is ignored. Let the initial angular velocity of the torsion pendulum beam be ω_0 , which can be obtained from the conservation of energy:

$$\frac{I\omega_0^2}{2} = \frac{Gmt^3 \alpha_{max}^2}{3l} \quad (3)$$

where α_{Max} is the maximum swing angle of the torsion pendulum in the first quarter period of motion.

Let the distance between the impulse action point and the axis of the C-shaped tube be L_s , which can be obtained from the conservation of the moment of momentum:

$$I_s L_s = I\omega_0 \quad (4)$$

By combining Eqs. (3) and (4):

$$I_s = \frac{\alpha_{max}}{L_s \sqrt{\frac{2Gmt^3 I}{3l}}} \quad (5)$$

Combining Eqs. (1) and (5), it can be seen that when the C-tube torsion pendulum is under the action of static force or impulse, its static force and impulse values are linear with the mechanical response of the system.

When the pendulum is stationary, the total length of the optical path from the circular mirror to the PDS is L , and the displacement of the light spot on the PDS is s when the pendulum is stationary to moving. The PDS can convert the displacement signal to the voltage signal V for output. Set the gain coefficient of PDS signal conversion as μ , then there are:

$$s = L \tan \alpha \quad (6)$$

$$V = \mu s \quad (7)$$

The relationship between voltage signal and impulse can be obtained from simultaneous formula (5)-(7) as follows:

$$I_s = \frac{V_{max}}{L_s \frac{1}{L\mu} \sqrt{\frac{2Gmt^3 I}{3l}} \frac{\alpha_{max}}{\tan \alpha_{max}}} \quad (8)$$

The impulse generated by the micro-nano satellite propulsion system is very small, corresponding to the maximum swing angle generated α_{Max} is smaller, at this time $\alpha_{max}/\tan \alpha_{max} \approx 1$. Therefore, formula (8) can be simplified as:

$$I_s = \frac{V_{max}}{L_s \frac{1}{L\mu} \sqrt{\frac{2Gmt^3I}{3l}}} \quad (9)$$

If $K = \frac{1}{L\mu} \sqrt{\frac{2Gmt^3I}{3l}}$, the K value can be determined by calibrating the torsion pendulum system, and then, the measurement impulse can be calculated by recording the maximum voltage V_{max} displayed on the PDS.

3.2 Calibration

The establishment of a highly sensitive micro-impulse measurement platform enables accurate measurement of the thrust and impulse of the micro-thruster. In order to accurately measure thrust and impulse and ensure that the system operates properly and performs well, the measuring system must be calibrated as accurately as possible. Calibration is a necessary step prior to all accurate measurements, and the accuracy of calibration directly affects the accuracy of the measurements system. There are many kinds of calibration methods, and more than one method of calibration for the same measurement system. The measurement system should use the calibration method as accurately as possible. The high-precision electromagnetic calibration technology based on pulsed ampere force uses the energized copper wire to pass through the magnetic field orthogonal to it to generate ampere force and uses this ampere force to act on the measuring bench as the calibration force, effectively solving the high-precision calibration problem of the C-tube torsion pendulum measuring device.

For a ring electromagnet, as shown in **Figure 5**, when the cross-sectional area and permeability of the electromagnet are the same everywhere, a magnetic circuit will be generated in the electromagnet and the magnetic lines of force will be basically concentrated in the magnetic core. When the air gap height is small, most of the magnetic force lines pass through the air gap, and only a few of the magnetic force lines are outside the air gap. In most areas of the air gap, the magnetic induction intensity is uniform, and at the edge of the air gap, the magnetic induction intensity drops rapidly. The software Ansoft is used to carry out a numerical simulation on the magnetic induction intensity of the air gap and its periphery, and the magnetic induction intensity distribution on the middle cross-section of the annular magnetic gap is obtained, as shown in **Figure 6**. In the simulation, the electromagnet material is silicon steel, the electromagnet coil is 200 turns, the energizing current is 0.5 A, the gap section area is, and the gap spacing is 2 mm. It can be seen from **Figure 6** that

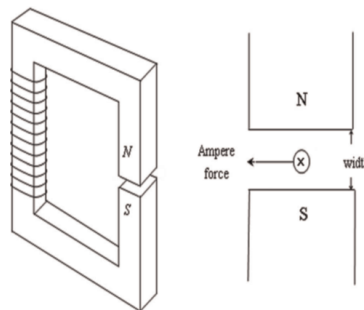


Figure 5.
Ampere force in annular magnet and gap.

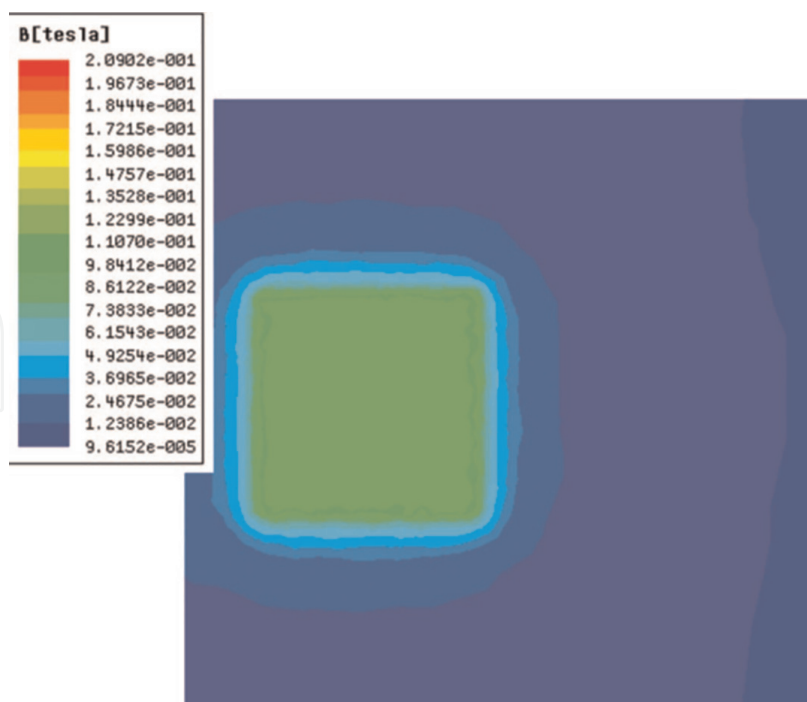


Figure 6.
 Distribution of magnetic induction intensity.

when the volume is $2 \times 15 \times 15 \text{ mm}^3$, the uniformity of magnetic induction intensity is satisfied.

In magnetic field B , the force on the current-carrying conductor can be expressed as

$$df = I_C \cdot dl \times B \quad (10)$$

Therefore, when the electrified straight wire is in the gap, it will be affected by the magnetic field. The force is called ampere force, that is, L is the effective length of the straight wire with current I_C in the uniform magnetic field with strength B .

$$F = BI_C L \quad (11)$$

Due to the edge effect of the magnetic field, it is difficult to calculate the ampere force through Eq. (11). However, when the magnetic field remains constant and L remains constant, the ampere force will be proportional to the coil current. In addition, when the current in the copper coil remains constant, the ampere force will be constant. As shown in **Figure 7**, the ampere force can be obtained by the physical analysis balance weighing method, and then it can be used as the calibration force. Different coil currents will correspond to different ampere forces for calibration. If there is a pulsed current in the coil, a pulsed ampere force will be generated between the coil and the magnetic field. By integrating the pulse ampere force with time, the impulse received by the copper coil can be obtained and then used as the impulse required for calibration.

Another advantage of this electromagnetic calibration method is that the ampere force is not sensitive to the angular displacement of the force arm. This is because the magnetic field is uniform in a large range of the electromagnet gap. Therefore, as long as the energized wire is not close to the edge of the gap, the generated ampere force will not be affected by the position of the copper wire. No matter how the position of

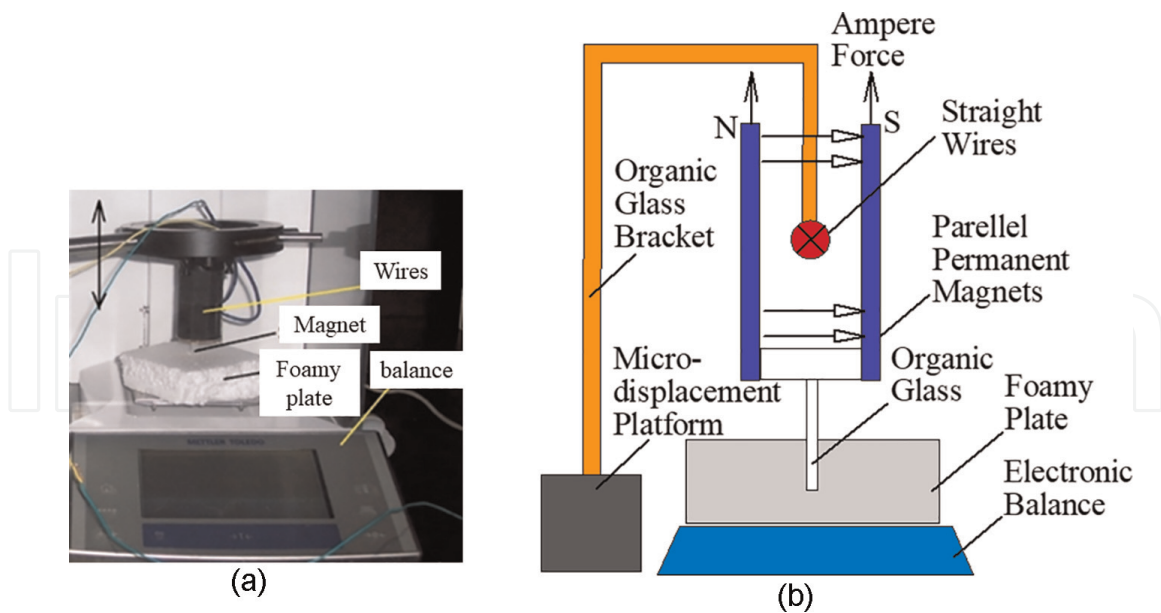


Figure 7. Measuring ampere force with physical analytical balance. (a) Physical measurement diagram (b) schematic diagram.

the copper wire changes, as long as the copper wire enters and exits from one side of the air gap, the ampere force will remain unchanged, thus ensuring the accuracy of the calibration process.

3.3 Electromagnetic compatibility technology

In the electronic circuit system, when there is a high-frequency circuit, the circuit will radiate electromagnetic waves to the outside, or some parts of the system use components that can radiate electromagnetic waves. These radiated electromagnetic waves will interfere with other nearby equipment and will be coupled to the circuit through wires and various connectors, causing interference to the signal in the circuit. There are also many elements with antenna functions in the circuit system, such as cables, printed circuit boards, and some mechanical structures. These elements can be coupled to other lines in the form of electric and magnetic fields, causing interference to the system. Electromagnetic compatibility (EMC) of equipment or system refers to the ability of equipment or system to work normally in an electromagnetic environment without causing unbearable electromagnetic interference to any other thing in the environment.

The project team has analyzed and studied the electromagnetic compatibility technology of the C-tube torsion pendulum micro-thrust/micro-impulse measuring device and processed the line shielding, grounding, lapping technology, and signal filtering technology for the system according to the actual situation, and finally carried out a comparative study of the influence of the electromagnetic compatibility technical measures on the measured signal of the system. The research results show that these processes reduce noise and improve the signal-to-noise ratio to a certain extent, but at the same time, it is also concluded that electromagnetic compatibility technology is not perfect, and it is difficult to completely eliminate noise and obtain clean measured signals by using electromagnetic compatibility technology alone. It is also necessary to filter the signal data by software, and the combination of the two can obtain more ideal signal data.

3.4 Experimental measurement

The thrust of the thruster with known parameters is measured to further verify the accuracy of the measurement method. The overall test device is shown in **Figure 8**. The thruster is installed on one side of the torsion pendulum. When the thruster works, its impulse will act on the torsion pendulum system. When the thruster works, its impulse will act on the swing arm and drive the torsion bar to rotate; The reflector installed on the swing arm reflects the laser beam emitted by the He-Ne laser to the remote PDS photosensitive surface; With the action of the impulse, the light spot produces a small displacement on the PDS photosensitive surface, which makes the PDS produce a small voltage signal output.

The measurement results of micro and thrusts and impulses are shown in **Tables 1** and **2**. According to the results in the table, this measuring device can realize the measurement of thrust and impulse of microns. At the same time, the resolution of PDS can be further improved and more sensitive materials can be selected to excavate higher resolution. In theory, this measuring device can achieve at least 100 nN and 100 nN·s measurements.

3.5 Error analysis

According to the possible error sources, the measurement error sources of the C-tube torsion pendulum are divided into the error introduced by the optical lever structure, the error introduced by the PDS sensor, and the error introduced by the acquisition card and the calibration error. The optical lever is used to measure the mechanical response of the C-tube torsion pendulum, and its structure affects the resolution of the C-tube torsion pendulum. PDS is a part of the optical lever and a sensor sensitive to the change of light spot displacement. Its resolution and optical path of the optical lever together determine the resolution of the C-tube torsion pendulum. The acquisition ability of the data acquisition card determines the system's ability to capture signals, and the acquisition accuracy of signals also affects the accuracy of the system's measurement results. Calibration is the basis for accurate measurement of C-tube torsion pendulum, and the calibration error introduced by calibration will be directly introduced into the measurement results. Other factors that may cause the measurement error of the system include the mechanical vibration of the system, the imperfection of the measuring circuit, and some undetected influencing factors. The mechanical vibration of the system will cause the vibration of the

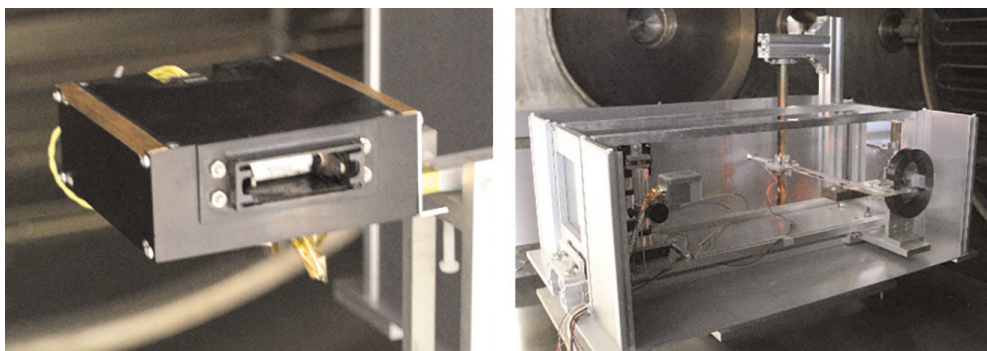


Figure 8.
Test device.

Theoretical thrust (μN)	Measuring voltage (V)	Measuring thrust (μN)
25	0.00116	26.721
50	0.00698	48.398
100	0.01860	104.487
150	0.03023	158.843
200	0.04186	211.273
250	0.01860	267.128
1250	0.11163	1208.676
2500	0.22790	2581.426
12,500	1.15814	12700.4687

Table 1.
Measuring results of thrusts.

Theoretical impulse ($\mu\text{N s}$)	Measuring voltage (V)	Measuring impulse ($\mu\text{N s}$)
10	0.04186	9.870
20	0.08837	20.345
40	0.18140	39.898
60	0.27742	62.448
80	0.36774	81.539
100	0.46065	107.352
500	2.32093	513.682
1000	4.64651	1089.613
5000	23.25116	5204.365

Table 2.
Measuring results of impulses.

C-tube, plane mirror, laser light source, and other structures of the system. The vibration of these structures will cause the vibration of the measuring optical path and cause low-frequency vibration interference to the measuring signal. The preliminary measurement circuit is not optimized, and the circuit itself may affect the quality of the measured signal, resulting in the reading error of the signal.

At the same time, the measuring range of the C-tube torsion pendulum is related to the machining accuracy and assembly accuracy when machining structural parts. For example, the beam and C-shaped tube, in order to ensure that the torsion pendulum has sufficient accuracy and resolution, the beam should have sufficient strength, and the processing should have good symmetry. When cutting an ordinary tube into a C-shaped tube, it should ensure sufficient cutting accuracy; otherwise, it will affect the mechanical properties of the C-shaped tube. During assembly, the structural dimension shall be measured before assembly. In the optical lever structure, the biggest influence on the measurement is the angle between PDS and incident light.

When the pendulum is still, PDS and incident light should be perpendicular, so the measurement model can be approximated as a linear model. Although this introduces method error, the relative error introduced by this approximation is very small. When the pendulum swing angle is 1 degree (actually far less than 1 degree), the relative error introduced by the approximation is about 0.1%. The relative position of the parallel plane mirror will affect the size of the system error. The larger the included angle of the plane mirror, the greater the system error caused, and of course, the greater the impact on the measurement results. Therefore, one of the mirrors can be installed on an adjustable platform, and the platform can be used to adjust the two mirrors close to the parallel state. The installation accuracy of the circular reflector does not need to be particularly high, but the connection between the circular reflector and the C-tube must be ensured to be tight enough.

4. Conclusion

Summarize the current status of micro-impulse measurement. To improve measurement accuracy, the following key technologies remain to be explored.

4.1 Environmental noise control technology

The system response measurement error caused by environmental noise interference is the dominant factor that causes thrust or impulse measurement errors. Therefore, environmental noise interference suppression technology is one of the key technologies for thrust or impulse measurement.

The challenge in suppressing environmental noise interference lies in its multi-source and diverse effects. Therefore, the research on the control technologies for environmental noise interference should focus on the identification of noise sources. These sources can be complex, including displacement hidden excitation interference, external force excitation interference, thrust or impulse loading interference, as well as the sight and drag interference caused by thruster connecting pipelines and cables, and the measurement error of displacement sensors.

4.2 High compensation system response measurement technology

The thrust or impulse is obtained from the inverse calculation of the measurement system response. The precision regarding the response of the measurement system will directly affect the accuracy of the thrust or impulse measurements. Therefore, high-precision system response measurement technology is one of the key technologies for thrust or impulse measurement.

The challenge of high-precision system response measurement is the measurement of small system response under environmental noise interference and small thrust-to-weight ratio. Spaceborne thruster (e.g., micro-thruster) has a very small thrust-to-weight ratio, which means that when carrying a thruster to measure thrust, the rotational inertia of the rotating parts of the measuring system is large, and the thrust that the thruster can generate is relatively small, so the displacement generated by thrust is very small, and there is also the impact of environmental noise interference, involving environmental noise interference and high-precision measurement of small displacement under small thrust-to-weight ratio.

4.3 High-precision calibration technology

Thrust or impulse measurement is to use the vibration differential equation of the measurement system to calculate thrust or impulse inversely. The calibration accuracy of system parameters will directly affect the accuracy of the thrust or impulse measurement. Therefore, high-precision system parameter calibration technology is one of the key technologies of thrust or impulse measurement. The difficulty of high-precision system parameter calibration is the suppression of environmental noise interference and the generation of high-precision constant force. In addition to the influence of environmental noise on the calibration accuracy of system parameters, the generation and acquisition method of high-precision constant force is an effective technical way to improve the calibration accuracy of system parameters.

4.4 High-precision evaluation technology

Thrust or impulse measurement is to give the measurement results of micro-thrust or impulse of millinewton (s) or even micro-newton (s) under the conditions of environmental noise interference suppression, micro-system response measurement, and high-precision system parameter calibration, as well as the evaluation conclusions with high confidence. Therefore, high-precision thrust or impulse measurement and evaluation technology is one of the key technologies of thrust or impulse measurement.

Acknowledgements

The authors would like to thank the Innovative Research Groups of the National Natural Science Foundation of China for the financial assistance provided under grant number T2221002 for this work.

Conflict of interest

The authors declare no conflict of interest.


IntechOpen

Author details

Yang Ou*, Yuqi Li, Yu Zhang, Jianjun Wu* and Yuqiang Cheng
College of Aerospace Science and Engineering, National University of Defense
Technology, Changsha, Hunan, China

*Address all correspondence to: ouyang16@nudt.edu.cn; jjwu@nudt.edu.cn

IntechOpen

© 2023 The Author(s). Licensee IntechOpen. This chapter is distributed under the terms of the Creative Commons Attribution License (<http://creativecommons.org/licenses/by/3.0>), which permits unrestricted use, distribution, and reproduction in any medium, provided the original work is properly cited. 

References

- [1] Levchenko I, Xu S, Teel G, Mariotti D, Walker MLR, Keidar M. Recent progress and perspectives of space electric propulsion systems based on smart nanomaterials. *Nature Communications*. 2018;**9**(1):879. DOI: 10.1038/s41467-017-02269-7
- [2] Levchenko I, Xu S, Mazouffre S, Lev D, Pedrini D, Goebel D, et al. Perspectives, frontiers, and new horizons for plasma-based space electric propulsion. *Physics of Plasmas*. 2020; **27**(2):020601. DOI: 10.1063/1.5109141
- [3] Levchenko I, Bazaka K, Ding Y, Raitses Y, Mazouffre S, Henning T, et al. Space micropropulsion systems for Cubesats and small satellites: From proximate targets to furthestmost frontiers. *Applied Physics Reviews*. 2018;**5**(1):011104. DOI: 10.1063/1.5007734
- [4] Dale E, Jorns B, Gallimore A. Future directions for electric propulsion research. *Aerospace*. 2022;**7**(9):120. DOI: 10.3390/aerospace7090120
- [5] Kang X, Liu J, Qiao C, Zhang Y. *Space Electric Propulsion Test Measurement Technology*. Beijing: Science Press; 2020 (in Chinese)
- [6] Wang M, Zhong X, Wang Y. *General Design of Electric Propulsion Spacecraft*. Beijing: Science Press; 2019 (in Chinese)
- [7] Zhang H, Li DT, Li H. Development of a cantilever beam thrust stand for electric propulsion thrusters. *Review of Scientific Instruments*. 2020;**91**(11):115104. DOI: 10.1063/5.0027911
- [8] Asakawa J, Nishii K, Nakagawa Y, Koizumi H, Komurasaki K. Direct measurement of 1-mN-class thrust and 100-s-class specific impulse for a CubeSat propulsion system. *Review of Scientific Instruments*. 2020;**91**(3):035116. DOI: 10.1063/1.5121411
- [9] James E, Anthony P. Recommended practice for thrust measurement in electric propulsion testing. *Journal of Propulsion and Power*. 2001;**33**(3):539-555. DOI: 10.2514/1.B35564
- [10] Ou Y, Zhang Y, Wu J, Tan S, Du X. Measurement method by inferring the thrust from the stress of the cantilever beam based on the photoelasticity theory. *Applied Optics*. 2019;**58**(36):9746. DOI: 10.1364/AO.58.009746
- [11] Wang D, Ye J, Li N, Wang Q, Wang J. A method of Micro-impulse measurement based on cantilever beam structure. *Instrument Technique and Sensor*. 2019;**3**(6):39-44. DOI: 10.3969/j.issn.1002-1841.2019.03.009
- [12] Ou Y. *Research on Thrust Measurement Method of Plasma Thruster Based on Stress Detection Technology*. Changsha: National University of Defense Technology; 2018 (in Chinese)
- [13] Mo X. *Research on Micro Bull Thrust Measurement Technology*. Chengdu: University of Electronic Science and Technology; 2019 (in Chinese)
- [14] Hong Y, Jin X, Ye J, Zhou W. *Microthrust and Microimpulse Measurement and Error Analysis Methods*. Beijing: Science Press; 2017 (in Chinese)
- [15] Hong Y, Li D, Feng X, Jin X, Wang S. *Measurement and Evaluation Methods for Propulsion Performance of Spaceborne Microthrusters*. Beijing: Science Press; 2021 (in Chinese)

- [16] Kakami A. Chapter 8 - thrust measurement. In: Cheah KH, editor. *Space Micropropulsion for Nanosatellites*. Elsevier; 2022. pp. 197-243. DOI: 10.1016/B978-0-12-819037-1.00010-4
- [17] Weng H, Cai G, Liu L, Zheng H, Zhang M, Zhang B. Modifying the theoretical model of the target indirect measurement method for measuring the thrust of electric propulsion. *Measurement Science and Technology*. 2021;**32**(8):085301. DOI: 10.1088/1361-6501/abe509
- [18] Wang B, Yang W, Tang H, Li Z, Kitaeva, et al. Target thrust measurement for applied-field magnetoplasmadynamic thruster. *Measurement Science and Technology* 2018;**29**:075302. DOI: 10.1088/1361-6501/aac079
- [19] Zhang H, Li DT, He F, Chen XW. Development of an indirect thrust stand based on a cantilever beam. *AIP Advances*. 2021;**11**(3):035006. DOI: 10.1063/5.0041530
- [20] Meng H, Lou J, Chen T, Xu C, Chen H, Yang Y, et al. Cantilever-based micro thrust measurement and pressure field distribution of biomimetic robot fish actuated by macro fiber composites (MFCs) actuators. *Smart Materials and Structures*. 2021;**30**(3):035001. DOI: 10.1088/1361-665X/abdaa9
- [21] Lu G. *Research on High Precision Micro Impulse Measurement Technology of PPT*. Changsha: National University of Defense Technology; 2014 (in Chinese)
- [22] Feng X, Hong Y, Cui H, Feng G. Numerical simulation and experimental research of high-precision electromagnetic calibration force. *Journal of Propulsion Technology*. 2021;**43**(8):1-18. DOI: 10.13675/j.cnki.tjjs.210806
- [23] Chang H, Ye J, Chen Y, Zhou W. Research on electromagnetic constant force characteristics for micro thrust measurement, infrared and laser engineering. *Infrared and Laser Engineering*. 2019;**6**:147-152. DOI: CNKI:SUN:HWYJ.0.2019-S1-021
- [24] Wang D, Jin X, Zhou W. Design and implementation of an electromagnetic force calibration device for micro thrust measurement, military automation. *Ordnance Industry Automation*. 2017;**36**:68-72. DOI: 10.7690/bgzdh.2017.09.017
- [25] Conde L, Lahoz MD, Grabulosa J, Hernández R, González J, Delgado M, et al. Thrust stand based on a single point load cell for impulse measurements from plasma thrusters. *Review of Scientific Instruments*. 2020;**91**(2):023308. DOI: 10.1063/1.5127189
- [26] Jarrige J, Thobois P, Blanchard C, Elias PQ, Packan D, Fallerini L, et al. Thrust measurements of the Gaia Mission flight-model cold gas thrusters. *Journal of Propulsion and Power*. 2014;**30**(4):934-943. DOI: 10.2514/1.B35091
- [27] Lun J, Law C. Direct thrust measurement stand with improved operation and force calibration technique for performance testing of pulsed micro-thrusters. *Measurement Science and Technology*. 2014;**25**(9):095009. DOI: 10.1088/0957-0233/25/9/095009
- [28] Phipps CR. A low-noise thrust stand for microthrusters with 25nN resolution. In: *AIP Conference Proceedings*. Nara (Japan): AIP; 2006. pp. 492-499. DOI: 10.1063/1.2203291
- [29] Koizumi H, Komurasaki K, Arakawa Y. Development of thrust stand

for low impulse measurement from microthrusters. *Review of Scientific Instruments*. 2004;75(10):3185-3190. DOI: 10.1063/1.1790568

[30] Yang YX, Tu LC, Yang SQ, Luo J. A torsion balance for impulse and thrust measurements of micro-Newton thrusters. *Review of Scientific Instruments*. 2012;83(1):015105. DOI: 10.1063/1.3675576

[31] Zhang D, Wu J, Zhang R, Zhang H, He Z. High precision micro-impulse measurements for micro-thrusters based on torsional pendulum and sympathetic resonance techniques. *Review of Scientific Instruments*. 2013;84(12):125113. DOI: 10.1063/1.4850615

IntechOpen